Structure of influenza haemagglutinin at neutral and at fusogenic pH by electron cryo-microscopy

Christoph Böttcher[a], Kai Ludwig[b], Andreas Herrmann[b], Marin van Heel[d], Holger Stark[c,e,*]

[a] *Freie Universität Berlin, Institut für Chemie/Forschungszentrum für Elektronenmikroskopie, Fabeckstr. 36a, D-14195 Berlin, Germany*
[b] *Humboldt-Universität zu Berlin, Math.-Nat. Fak. I, Institut für Biologie/Biophysik, Invalidenstr. 43, D-10115 Berlin, Germany*
[c] *Fritz-Haber-Institut, Max-Planck-Gesellschaft, Faradayweg 4-6, D-14195 Berlin, Germany*
[d] *Imperial College of Science, Medicine and Technology, Wolfson Laboratories, Department of Biochemistry, London SW7 2AY, UK*
[e] *Institut für Molekularbiologie und Tumorforschung, Emil-Mannkopff-Strasse 2, D-35037 Marburg, Germany*

Received 1 October 1999; received in revised form 20 October 1999

Edited by Hans-Dieter Klenk

Abstract The three-dimensional structures of the *complete* haemagglutinin (HA) of influenza virus A/Japan/305/57 (H2N2) in its native (neutral pH) and membrane fusion-competent (low pH) form by electron cryo-microscopy at a resolution of 10 Å and 14 Å, respectively, have been determined. In the fusion-competent form the subunits remain closely associated preserving typical overall features of the trimeric ectodomain at neutral pH. Rearrangements of the tertiary structure in the distal and the stem parts are associated with the formation of a central cavity through the entire ectodomain. We suggest that the cavity is essential for relocation of the so-called fusion sequence of HA towards the target membrane.

Key words: Electron microscopy; Fusion; Influenza; Hemagglutinin; Structure

1. Introduction

Influenza virus enters the host cell via receptor-mediated endocytosis [1]. The integral membrane protein haemagglutinin (HA) of influenza virus mediates fusion of the viral and endosomal membranes. HA is organised as a trimer of three 84 kDa monomers, each containing two disulphide linked subunits, HA1 and HA2. HA is anchored to the viral membrane via the C-terminus of HA2. The acidic pH in the endosome triggers a conformational change of the haemagglutinin ectodomain [1] which activates the fusion capacity [2,3]. The three-dimensional structure of the bromelain-cleaved ectodomain of HA (subtype H3) at neutral pH is already known from X-ray crystallography at a resolution of 3 Å [4]. The first 20 amino acids of the N-terminus of HA2 – the so-called 'fusion sequence' – are located at a distance of 35 Å from the viral membrane, oriented towards the trimer interface. While attempts to crystallise the ectodomain after its exposure to low pH failed, significant progress in understanding the spatial structure of this conformation was provided recently by studies with synthetic peptides [5] and from the X-ray crystal structure of fragments of the ectodomain obtained after several enzymatic treatments of HA (H3) upon acidification [6,7]. These studies suggest a 'spring-loaded' conformational change in that the loop of the HA2 subunit connecting two α-helices in the neutral form becomes now part of an extended trimeric coiled coil, thereby moving the fusion sequence to the tip of HA towards the target membrane. A 180° turn reorients the remaining C-terminus antiparallel towards the triple stranded coiled coil implying the colocalisation of the fusion sequence and the membrane anchor at one end of this rod-like structure [7,8]. Similar motives of a rod-like structure have been found for ectodomain fragments of the fusion proteins of other viruses and the SNARE complex involved in synaptic fusion (for review see [8]).

Mutations in the coiled coil region support the relevance of the spring-loaded conformational change for HA-mediated fusion [9]. However, previous studies strongly imply that other domains of HA must reorientate for fusion activation [1,10,11]. To unravel those structural alterations as well as the conformational pathway leading to the fusion active conformation the three-dimensional (3D) structure of the *intact* HA has to be determined. Here, by employing electron cryo-microscopy and image reconstruction, we present the 3D structure of intact HA upon activation of its fusion capacity. This structure serves to develop a model for the relocation of the fusion sequence towards the target membrane.

2. Materials and methods

2.1. Preparation of influenza virus

Influenza virus A/Japan/305/57 (H2N2) was grown for 48 h in the allantoic cavity of 10 days embryonated hen eggs and purified [12]. Fusion of influenza virus A/Japan/305/57 with erythrocyte ghost membranes was measured by fluorescence dequenching of the lipid-like fluorophore octadecylrhodamine B chloride (R18, Molecular Probes, Eugene, OR, USA) initially incorporated into the viral membrane at selfquenching concentration (approx. 2 mol% of total viral lipid) as described [13,14].

2.2. Isolation of HA

Twenty mg virus was solubilised in 2.5 ml phosphate buffered saline, 150 mmol/l NaCl (PBS), pH 7.4, containing 140 mg octylglycoside (Alexis Corporation, Läutelfingen, Switzerland) by shaking on ice for 1 h [12]. After centrifugation for 60 min at $100\,000 \times g$, the supernatant containing the HA in detergent micelles was purified by affinity chromatography on ricin A (Sigma Chemical Corporation, Deisenhofen, Germany). To remove the detergent and galactose 1 vol of sample was dialysed against 500 vol PBS and the purity of the HA was verified by SDS-PAGE. In the course of our study it was found to be advantageous to limit the dialysis to 15 min, thus keeping the number of HA trimers per rosette relatively low.

2.3. Electron cryo-microscopy

The rosettes of HA trimers were diluted 1:10 either with PBS (pH 7.4) or with a sodium acetate buffer (pH 4.9) and incubated for 10 min

*Corresponding author. Fax: (49)-6421-286 7008.
E-mail: stark@imt.uni-marburg.de

PII: S0014-5793(99)01475-1

at 4°C. Contrast material (1% PTA) was added to the rosette solutions, applied to electron microscopy grids and immediately vitrified by plunging into liquid ethane [15]. The PTA solution used in all cases was adjusted to pH 7.4 to avoid any pH dependent effect of PTA on the HA structure. A Gatan specimen holder/cryo-transfer system was used to image the samples in a Philips CM12 microscope under low dose conditions, at −174°C, using a primary magnification of 58300× and a defocus value corresponding to a first zero of the CTF at ∼8.5 Å (neutral pH) and ∼12 Å (low pH) respectively. Although our EM specimen preparation procedures are essentially the same as used for conventional cryo-microscopy [16] we have added Phospho-Tungstic-Acid to the sample on the grid. By that we obtained an embedding matrix with a somewhat higher contrast than conventional vitreous ice, allowing one to localise the particles in the micrographs even when the microscope is operated relatively close to focus.

2.4. Reconstruction of 3D structure of HA

Good electron micrographs (verified by optical diffraction) were digitised using the Image Science Software GmbH checkerboard densitometer with a pixel size corresponding to 2.2 Å on the specimen scale. All image processing was performed with the IMAGIC-5 software system [17] on SUN and DEC-alpha workstations. The HA trimers were extracted from the digitised micrographs (2928 and 1833 trimers at neutral and acidic pH, respectively) as 90×90 fields and these images pre-processed by standard procedures were submitted to multi-reference alignment [18], MSA data compression and automatic classification [19] to yield noise-free projection images. Using the 'angular reconstitution' technique [20] Euler angles were assigned to each of the projection images and a preliminary three-dimensional reconstruction was obtained. Iterative refinement procedures [21] were then applied leading to the final 3D reconstruction. The resolution in the reconstructions was assessed by separating the final class averages into two groups and using these groups to generate two different 3D reconstructions which were compared over corresponding shells in Fourier space (Fourier Shell Correlation). The 3σ threshold criterion curve was multiplied by the value $\sqrt{3} = 1.73$ to account for the C_3 pointgroup symmetry assumed during the processing which makes that only one third of the 3D Fourier space volume was independent [22]; the final resolutions were thus estimated to be ∼10 Å for the neutral pH 3D reconstruction and ∼14 Å for the pH 4.9 reconstruction. For the present 3D reconstructions the information up to the first zero of the contrast transfer function (CTF) was taken into account. The relative amplitudes of the spatial frequencies were normalised in order to avoid the unproportional representation of the signal in Fourier space. The combination of the electron microscopic imaging parameters and data analysis procedures (cf. filtering) yielded radial amplitude spectrum distributions which were quite similar to that of the X-ray map; this fact is reflected in the close similarity between the surface rendered images (Fig. 2).

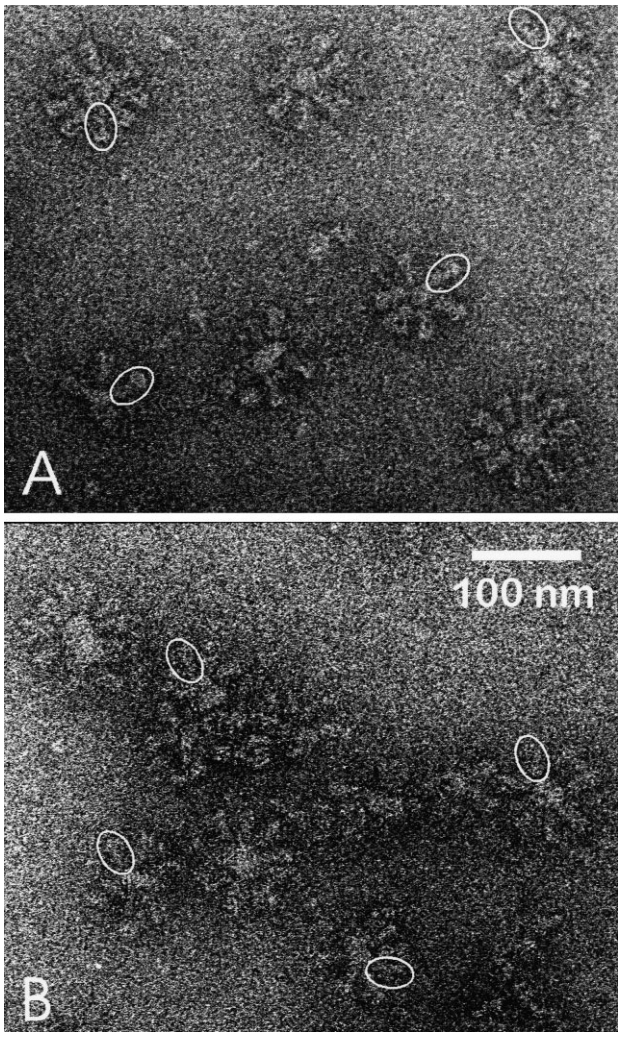

Fig. 1. Electron micrographs of influenza haemagglutinin (HA). HA trimer rosettes were isolated from influenza virus (strain A/Japan/305/57 (H2N2)) and embedded in a matrix of vitreous ice containing Phospho-Tungstic-Acid (PTA, 1% (w/v)). A: After incubation for 10 min at 4°C at neutral pH (7.4). B: After incubation for 10 min at 4°C at low pH (4.9) where HA is in a conformation that can trigger fusion of viral and host membranes. Individual trimers of HA are encircled in white.

3. Results

3.1. 3D structure of HA at neutral pH

We have isolated HA from influenza virus A/Japan/305/57 (H2N2) [23], which maintains its fusion potential upon prolonged incubation at acidic pH [24]. In contrast, often used strains of influenza A virus such as X31 (H3) and A/PR 8/34 (H1) may rapidly inactivate at low pH in the absence of target membranes [11,25–27]. Upon removal of detergent, HA trimers associate into 'rosettes' [28,29] in which their various orientations can be exploited in order to reconstruct the three-dimensional structure from electron microscopical images. The rosette samples were incubated either at neutral pH (7.4) or at acidic pH (pH 4.9) and subsequently prepared for cryo-microscopy (Fig. 1).

Trimers were selected interactively from the digitised micrographs and, after alignment, similar images were averaged into classes of 'characteristic views'. The Euler orientations of these relatively noise-free projection images were determined by angular reconstitution [20] under the constraint of C3 symmetry. The resulting neutral pH ectodomain structure at a resolution of 10 Å is depicted in Fig. 2A. (The anchoring of the transmembrane domain within the central lipid mass of the rosettes remains unresolved and has therefore been excluded from the reconstruction procedure.) This structure is in excellent agreement with the known X-ray crystallographic structure (Fig. 2B) of the bromelain-cleaved ectodomain of HA from influenza X31 [4]. The length (∼135 Å) of the ectodomain and the diameter of its top region (∼60 Å) are almost identical. Close to the 3-fold axis in the EM reconstruction, structural details can be identified (Fig. 3A, B) to correspond to the triple coiled coil known from the X-ray structure [4]. Some minor differences exist between the EM reconstruction and the X-ray map (arrows in Fig. 2).

The *first* conclusion to be drawn from this remarkable similarity is that the combination of specimen preparation (vitreous ice embedding including PTA), close to focus cryo-microscopy, and the angular reconstitution computational

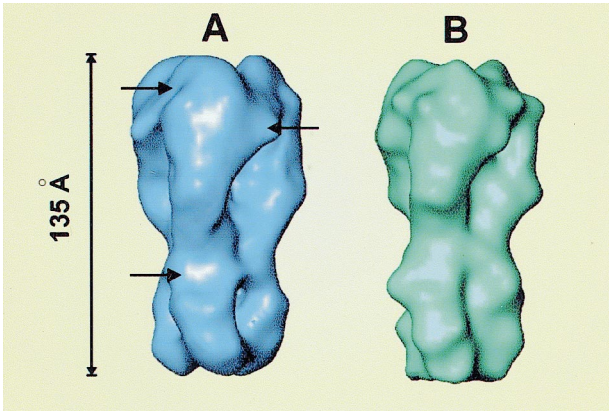

Fig. 2. The 3D structure of the haemagglutinin trimer at neutral pH. 3D reconstruction of the ectodomain of the influenza haemagglutinin trimer (A/Japan/305/57 (H2N2)) at neutral pH determined from cryo-electron micrographs (A) in comparison to the X-ray structure (4), low-pass filtered in order to provide a comparable resolution level (B). Small differences between the X-ray and the EM structure are indicated by arrows. The resolution of the EM structure, calculated from 2928 individual trimers, is ~10 Å as determined by Fourier Shell Correlation. Whereas in the X-ray structure the membrane region was cleaved off by bromelain treatment, this part of the protein was included into the EM reconstruction, but is not resolved due to lack of contrast caused by the neighbourhood of lipids. The viral membrane, which is not shown in the representation, would then be located at the lower end of the haemagglutinin trimer in a distance of 18 Å.

procedures is indeed capable of elucidating the 3D structure of such membrane proteins with great fidelity. The *second* conclusion is that the 3D structure of the native ectodomain of different HA subtypes is very similar. So far the structure of the ectodomain of only one virus strain (H3, X31) was known. The *third* conclusion is that our study confirms that the HA ectodomain in the X-ray crystallographic structure [4] has indeed not been affected by the bromelain cleavage of the transmembranes and the intraviral HA domains.

3.2. 3D structure of HA at acidic pH

Having established the reliability of our methodology, we now turn to the main goal of our investigations, the conformation of the trimeric ectodomain at acidic pH (4.9). Under this low pH condition, significant fusion of influenza virus A/Japan/305/57 with erythrocyte membranes can be observed even at 4°C (results not shown) and no indication of any low pH mediated inactivation of the fusion potential can be detected [11]. The homogeneity of the population was an essential precondition for a successful three-dimensional reconstruction, since the image processing procedure requires projection images of the molecules in a well-defined structural state. Thus, we here study the three-dimensional low pH structure of the complete ectodomain of the intact HA trimer in a defined and fusion-competent state, not cleaved enzymatically or in any other way compromised by the necessity to grow crystals. The resulting structure, at a current resolution

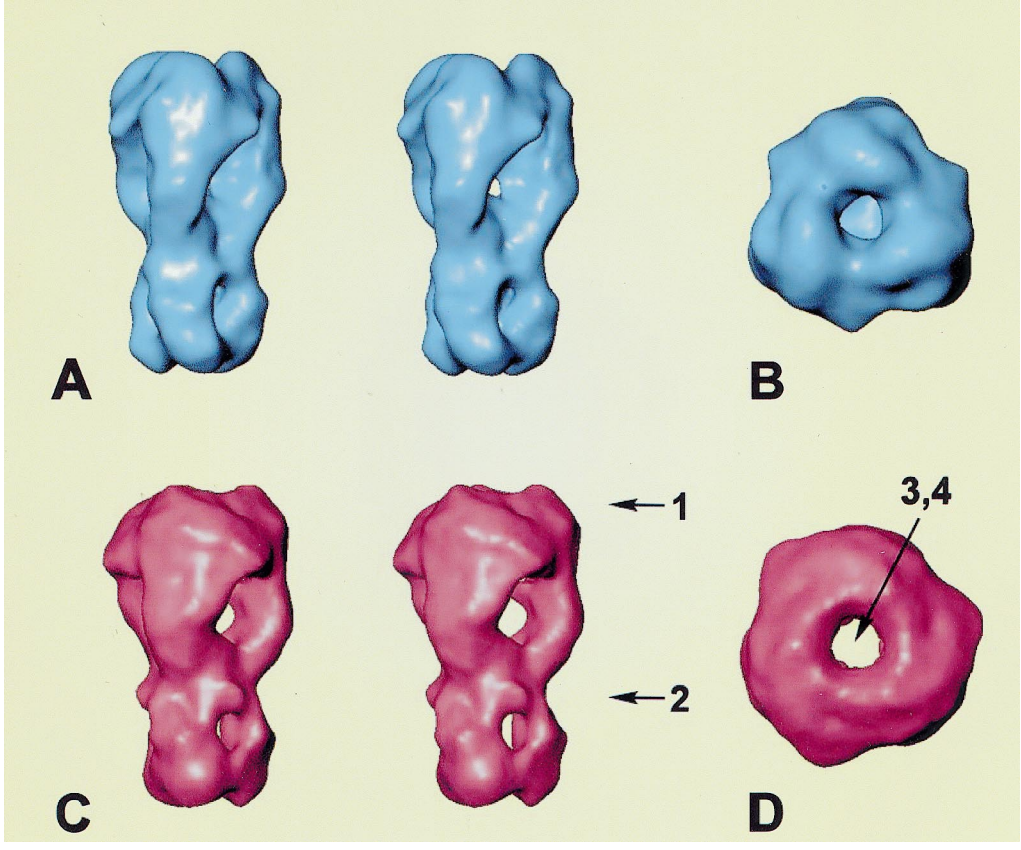

Fig. 3. The 3D structure of the fusion-competent haemagglutinin trimer. Stereo views of 3D reconstructions determined from cryo-electron micrographs of the trimeric ectodomain of influenza haemagglutinin (A/Japan/305/57 (H2N2)) at neutral pH (A) and at low pH (pH 4.9) (C). The most significant differences of the two conformational states of haemagglutinin are indicated by numbers: (1) a flattening of the top of the distal domains, (2) a torsion of the ectodomain mainly in the part located above the membrane, (3) a refolding of the stem region of the trimer, and (4) the formation of a continuous central cavity through the whole trimer (B, D).

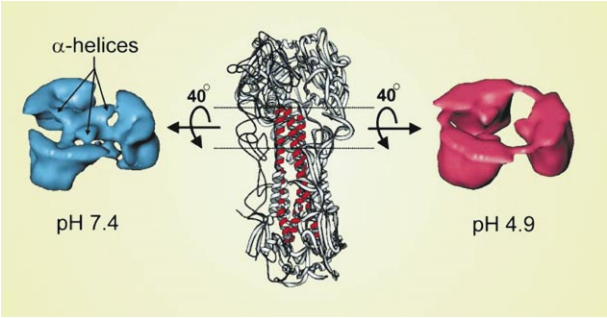

Fig. 4. Acidification causes distinct alterations in the HA ectodomain. Changes in the ectodomain of influenza haemagglutinin HA (pH 7.4) upon acidification to pH 4.9 are revealed by extracting a slice from each of the reconstructions. The relevant area is indicated by dotted lines in the secondary structure representation of the X-ray data at neutral pH (PDB ID: 2HMG), centre of the figure. The extracted parts of both EM structures were rotated about 40° to visualise differences which occur in the stem region between neutral (left) and low pH (right) conformation. Upon acidification, the absence of the α-helices at the pH 7 position becomes evident.

of 14 Å, is shown in Fig. 3C, D. The first impression conveyed by this 3D map is its similarity to the neutral pH one. The subunits of the trimer remain closely associated preserving typical overall features of the ectodomain at neutral pH (cf. Fig. 3A and C). However, upon closer inspection, various significant differences between the two EM structures become apparent, which are large compared to the marginal differences between the neutral pH structures by EM and by X-ray crystallography, respectively. The most significant distinctions are: (i) a flattening of the top of the distal domains, (ii) a torsion of the ectodomain mainly in the part located above the membrane, (iii) a refolding of the stem region of the trimer, and (iv) the formation of a continuous central cavity through the whole trimer.

4. Discussion

We have employed the angular reconstitution/cryo-microscopy approach for the 3D reconstruction of intact HA in two distinct conformations, in its native (neutral pH) and fusion-competent (acidic pH) state. With the achieved resolution of 10 Å and 14 Å, respectively, detailed changes of the ectodomain are detected which allow firm conclusions on this fusion-competent structure. A striking feature of the fusion-competent structure, confirming recent suggestions [6,24, 30,31], is that the subunits of the trimer remain tightly connected. No de-trimerisation, i.e. opening of the HA1 membrane-distal domain can be observed. Most surprisingly, a central cavity or 'channel' through the entire ectodomain has been found for the complete HA at low pH (Fig. 3). The observed torsion of the monomers close to the membrane surface causes a widening of the trimer interior reminding one of an 'iris diaphragm' mechanism. Structural elements, which represent helical parts of HA2, disappeared from the centre of the ectodomain at neutral pH (Fig. 4). However, the 3D density map implies the reorientation of this central density away from the trimer axis, towards the periphery of the ectodomain. The N-terminus of the HA2 may also be turned outwards from the subunit interface giving rise to an enhanced flexibility of the HA2 subunit. We cannot preclude that due to its hydrophobic properties, this segment remains associated with the trimer surface upon its exposure rather than to project out of the trimer.

Torsion is paralleled by alterations of the HA1 membrane-distal globular domain. It is very likely that inhibition of this domain's flexibility would prevent the formation of the cavity, and thus fusion. Indeed, cross-linking the membrane-distal domain via disulphide bonds abolishes membrane fusion [32,33]. We surmise that the cavity or 'channel' is an essential characteristic of the fusion-competent conformation.

This fusion-competent structure is different from the well-defined extended coiled coil, rod-like structure of HA2 fragments [6,34]. An elongated structure of HA, like the extended triple stranded coiled coil, could have been easily identified by our approach. Although our low pH structure does not necessarily suggest such conformational changes, very likely it is an intermediate structure enabling the contact with the target membranes via the hydrophobic HA sequences becoming exposed. The structure could then still transfer into the low pH conformation proposed by Wiley and coworkers [6,7,34] upon interaction with the lipid phase of the target membrane. In particular, the continuous cavity (Fig. 3) within the trimer might facilitate the relocation of the 'fusion peptide'. It was found that the loop region between the two α-helices of the neutral pH form remains highly flexible at low pH [35]. Both the flexibility of the loop region and the cavity may give rise to conformational alterations facilitating the relocation of the fusion peptide towards the tip of the ectodomain, the site of the target membrane. In this way, the transient association of the HA1 globular domains and the cavity represent essential features of the fusion-competent structure. Eventually, in the presence of the target membrane, the formation of the extended trimeric coiled coil enables the insertion of the fusion peptide into [36] and destabilisation of the target membrane. According to our data and as suggested very recently [31], the coiled coil is likely to represent the final state of the low pH mediated conformational transitions of the ectodomain, but not the precursor of fusion.

Based on low resolution cryo-electron microscopy a three-state model has been suggested which relates the conformational transitions of HA to the mechanism of viral fusion [24,37,38]. According to this model, HA undergoes a proton-driven shift from a 'T' (tense) state at neutral pH, to a state maintaining the typical spike morphology of HA trimers. This metastable state which is relaxed with respect to the T state was termed 'R'. It was followed by a transition to the 'D' (desensitised) state for which a fuzzy morphology is characteristic. Independent evidence was given that the R state resembles a fusion active conformation of HA, while the D state resembles an inactivated structure [24,35]. In line with that, Shangguan and coworkers [31] recently showed that inactivation of A/PR/8/34 HA at pH 4.9 correlated with loss of spike morphology as determined by cryo-electron microscopy. Very likely, the fusion-competent structure identified here by 3D cryo-microscopy reflects the R state.

We propose that the HA1 domain does not only prevent the conformational change of the HA2 subunit at neutral pH [5], but it also controls the conformational change of HA2 at low pH to enable fusion. This supports a very recent study of Gray and Tamm [39] which suggested a key role of HA1 at acidic pH for correct orientation of HA2 with respect to the target membrane enabling fusion. Presumably, the transient

stability of the association of the HA1 membrane-distal domains is an important factor retarding the inactivation of influenza virus at low pH, too. Dissociation of the domains exposes the fusion sequence with its strong hydrophobic properties [40]. Coiled coil structures with an exposed hydrophobic fusion sequence at the tip immediately tend to aggregate and/or insert into the viral membrane in the absence of a target membrane [41,42]. This would drive the ectodomain into a fusion inactivated conformation. Thus, membrane fusion requires a distinct sequence of conformational changes of viral fusion proteins. This sequence is determined by the structure of the fusion protein as well as the presence of the target membrane. Substances which inactivate fusion irreversibly by disturbing the sequence of conformations at low pH are attractive candidates to prevent influenza virus infection [43]. Notably, aggregation of HA trimers impairs our approach since trimers can no longer be treated as single particles in the image processing procedure. Therefore, we regard it as very difficult to identify the coiled coil conformation of the intact HA in the absence of the target membrane.

The angular reconstitution/cryo-microscopy approach is used here for the first time to elucidate the 3D structure of a relatively small membrane-anchored protein in different conformational states. The resolution of 10 Å attained is one of the highest achieved by single particle analysis to date. Bearing in mind that a standard electron cryo-microscope with a thermionic electron source, rather than a highly coherent Field Emission Gun, was used in our study, it is obvious that there remains substantial room for improvement towards higher resolution.

Acknowledgements: This work was supported by grants of the Deutsche Forschungsgemeinschaft to C.B., A.H., and M.v.H. We thank Dr. Michael Schatz and Ralf Schmidt of Image Science GmbH for software support, and Bärbel Hillebrecht for expert technical assistance.

References

[1] White, J.M. and Wilson, I.A. (1987) J. Cell Biol. 105, 2887–2896.
[2] Maeda, T. (1980) FEBS Lett. 122, 283–287.
[3] Huang, R.T.C., Rott, R. and Klenk, H.-D. (1981) Virology 110, 243–247.
[4] Wilson, I.A., Skehel, J.J. and Wiley, D.C. (1981) Nature 289, 366–373.
[5] Carr, C.M. and Kim, P.S. (1993) Cell 73, 823–832.
[6] Bullough, P., Hughson, F.M., Skehel, J.J. and Wiley, D.C. (1994) Nature 371, 37–43.
[7] Chen, J., Skehel, J.J. and Wiley, D.C. (1999) Proc. Natl. Acad. Sci. USA 96, 8967–8972.
[8] Skehel, J.J. (1998) Cell 95, 871–874.
[9] Qiao, H., Pelletier, S.L., Hoffman, L., Hacker, J., Armstrong, R.T. and White, J.M. (1998) J. Cell Biol. 141, 1335–1347.
[10] Steinhauer, D.A., Martin, J., Lin, Y.P., Wharton, S.A., Oldstone, M.B.A., Skehel, J.J. and Wiley, D.C. (1996) Proc. Natl. Acad. Sci. USA 93, 12873–12878.
[11] Korte, T., Ludwig, K., Krumbiegel, M., Zirwer, D., Damaschun, G. and Herrmann, A. (1997) J. Biol. Chem. 272, 9764–9770.
[12] Krumbiegel, M., Herrmann, A. and Blumenthal, R. (1994) Biophys. J. 67, 2355–2360.
[13] Hoekstra, D., de Boer, T., Klappe, K. and Wilschut, J. (1984) Biochemistry 23, 5675–5681.
[14] Herrmann, A., Clague, M.J. and Blumenthal, R. (1993) Biophys. J. 65, 528–534.
[15] Böttcher, C., Stark, H. and van Heel, M. (1996) Ultramicroscopy 62, 133–139.
[16] Adrian, M., Dubochet, J., Lepault, J. and Mc Dowell, A.W. (1984) Nature 308, 32–36.
[17] van Heel, M., Harauz, G., Orlova, E.V., Schmidt, R. and Schatz, M. (1996) J. Struct. Biol. 116, 17–24.
[18] van Heel, M. and Stöffler-Meilicke, M. (1985) EMBO J. 4, 2389–2395.
[19] van Heel, M. (1989) Optik 82, 114–126.
[20] van Heel, M. (1987) Ultramicroscopy 21, 111–124.
[21] Schatz, M., Orlova, E.V., Dube, P., Jäger, J. and van Heel, M. (1995) J. Struct. Biol. 114, 28–40.
[22] Orlova, E.V., Dube, P., Harris, J.R., Beckmann, E., Zemlin, F., Markl, J. and van Heel, M. (1997) J. Mol. Biol. 271, 417–437.
[23] Doms, R., Helenius, A. and White, J. (1985) J. Biol. Chem. 260, 2973–2981.
[24] Puri, A., Booy, F.P., Doms, R.W., White, J.M. and Blumenthal, R. (1990) J. Virol. 64, 10108–10113.
[25] White, J., Kartenbeck, J. and Helenius, A. (1982) EMBO J. 1, 217–222.
[26] Stegmann, T., Booy, F.P. and Wilschut, J. (1987) J. Biol. Chem. 262, 17744–17749.
[27] Nir, S., Düzgünes, N., Pedroso de Lima, M. and Hoekstra, D. (1990) Cell Biophys. 17, 181–201.
[28] Kawasaki, K., Sato, S. and Ohnishi, S. (1983) Biochim. Biophys. Acta 733, 286–290.
[29] Ruigrok, R.W., Martin, S.R., Wharton, S.A., Skehel, J.J., Bayley, P.M. and Wiley, D.C. (1986) Virology 155, 484–497.
[30] Stegmann, T., White, J. and Helenius, A. (1990) EMBO J. 9, 4231–4241.
[31] Shangguan, T., Siegel, D.P., Lear, J.D., Axelsen, P.H., Alford, D. and Bentz, J. (1998) Biophys. J. 74, 54–62.
[32] Godley, L., Pfeifer, J., Steinhauer, D., Ely, B., Shaw, G., Kaufmann, R., Suchanek, E., Pabo, C., Skehel, J.J., Wiley, D.C. and Wharton, S. (1992) Cell 68, 635–645.
[33] Kemble, G.W., Bodian, D.L., Rose, J., Wilson, I.A. and White, J.M. (1992) J. Virol. 66, 4940–4950.
[34] Skehel, J.J., Bizebard, T., Bullough, P.A., Hughson, F.M., Knossow, M., Steinhauer, D.A., Wharton, S.A. and Wiley, D.C. (1995) Cold Spring Harb. Symp. Quant. Biol. 60, 573–580.
[35] Kim, C.-H., Macosko, J.C., Yeon Gyu, Yu. and Shin, Y.-K. (1996) Biochemistry 35, 5359–5365.
[36] Lüneberg, J., Martin, I., Nüssler, F., Ruysschaert, J-M. and Herrmann, A. (1995) J. Biol. Chem. 270, 27606–27614.
[37] Blumenthal, R., Puri, A., Sarkar, D.P., Chen, Y., Eidelman, O. and Morris, S.J. (1989) in: Cell Biology of Virus Entry, Replication and Pathogenesis (Helenius, A., Compans, R. and Oldstone, M., Eds.), pp. 197–217, Alan Liss, Inc, New York.
[38] Korte, T., Ludwig, K., Booy, F.P., Blumenthal, R. and Herrmann, A. (1999) J. Virol. 73, 4567–4574.
[39] Gray, C. and Tamm, L. (1997) Protein Sci. 6, 1993–2006.
[40] Durell, S.R., Martin, I., Ruysschaert, J.-M., Shai, Y. and Blumenthal, R. (1997) Mol. Membr. Biol. 14, 97–112.
[41] Wharton, S.A., Calder, L.J., Ruigrok, R.W.H., Skehel, J.J., Steinhauer, D.A. and Wiley, D.C. (1995) EMBO J. 14, 240–246.
[42] White, J.M. (1995) Cold Spring Harb. Symp. Quant. Biol. 60, 581–588.
[43] Hoffman, L.R., Kuntz, I.D. and White, J.M. (1997) J. Virol. 71, 8808–8820.